UDC 550.34.01:504.3.054

R.B. Nuterman[1,2], *Ph.D.*, **A.A. Baklanov**[1], *Prof., Sc.D.*, **A.V. Starchenko**[2], *Prof., Sc.D.*
[1]*Danish Meteorological Institute, Copenhagen, Denmark*
[2]*Tomsk State University, Tomsk, Russia*

APPLICATION OF MICROSCALE MODEL FOR DEVELOPMENT OF URBAN CANOPY PARAMETRIZATION SCHEME FOR MESOSCALE MODELS

Abstract. *A numerical simulation of flows in urban canopy is important from the view point of emergency preparedness and development of new schemes for parameterization of atmospheric boundary layer in NWP. This study performs the analysis of spatial averaged properties of flow around different urban like obstacles.*

Keywords: *obstacle resolved microscale model, urban canopy parameterization.*

1 Introduction

Prediction and understanding of basic physical phenomena of complex flows in and above the urban canopy provide not only prevention of potential ecological risks but promote the development of new schemes for parameterization of urban areas for numerical weather prediction models. Recently, many scientists attend to investigation of aerodynamics and pollution transport in arrays of cubes/obstacles [4, 6]. These obstacles model buildings that are elements of the urban roughness. The arrangement and size of buildings are very changeable in reality. Therefore, estimation of impact of the geometry variation is important.

The goal of the study is investigation of aerodynamics in array of obstacles and the analysis of averaged flow variables.

2 Methodology and Data

We assume that the flow is incompressible and influence of body force is insignificant. The modeling of aerodynamics is based on Reynolds averaged Navier-Stokes equations [8]:

$$\frac{\partial \overline{u}_j}{\partial x_j} = 0\,,$$

$$\frac{\partial \overline{u}_i \overline{u}_j}{\partial x_j} = -\frac{1}{\rho}\frac{\partial \overline{p}}{\partial x_i} + \nu \frac{\partial}{\partial x_j}\left(\frac{\partial \overline{u}_i}{\partial x_j}\right) - \frac{\partial}{\partial x_j}\left(\overline{u_i' u_j'}\right),\ i = 1,2,3\,, \qquad (1)$$

where $\overline{u}_i$ is the averaged projection of the velocity vector on axis Ox_i; $\overline{p}$ is the pressure; ρ is the density; ν is the kinematic viscosity; $\overline{u_i' u_j'}$ is the Reynolds stresses.

The turbulence closure of the averaged momentum equations is based on the two-equation *k*-ε model of turbulence with non-linear dependence of the eddy viscosity on component of strain rate and vorticity tensors (non-linear eddy-viscosity model, NLEVM) [2]:

$$\overline{u}_j \frac{\partial k}{\partial x_j} = \frac{\partial}{\partial x_j}\left[\left(\nu + \frac{\nu_T}{\sigma_k}\right)\frac{\partial k}{\partial x_j}\right] + P - \varepsilon\,, \qquad (2)$$

$$\overline{u}_j \frac{\partial \varepsilon}{\partial x_j} = \frac{\partial}{\partial x_j}\left[\left(\nu + \frac{\nu_T}{\sigma_\varepsilon}\right)\frac{\partial \varepsilon}{\partial x_j}\right] + (c_{\varepsilon 1} P - c_{\varepsilon 2}\varepsilon)\frac{\varepsilon}{k}, \tag{3}$$

$$\begin{aligned} a_{ij} = \overline{u_i' u_j'}\,/k - 2/3\,\delta_{ij} = -\nu_T/k\, S_{ij} + C_1 \nu_T/\varepsilon\left(S_{ik}S_{kj} - 1/3\, S_{kl}S_{kl}\delta_{ij}\right) + \\ + C_2 \nu_T/\varepsilon\left(\Omega_{ik}S_{kj} + \Omega_{jk}S_{ki}\right) + C_3 \nu_T/\varepsilon\left(\Omega_{ik}\Omega_{jk} - 1/3\,\Omega_{kl}\Omega_{kl}\delta_{ij}\right) + \\ + C_4 \nu_T k/\varepsilon^2\left(S_{ki}\Omega_{lj} + S_{kj}\Omega_{li}\right)S_{kl} + \\ + C_5 \nu_T k/\varepsilon^2\left(\Omega_{il}\Omega_{lm}S_{mj} + S_{il}\Omega_{lm}\Omega_{mj} - 2/3\, S_{lm}\Omega_{mn}\Omega_{nl}\delta_{ij}\right) + \\ + C_6\, \nu_T k/\varepsilon^2\, S_{ij}S_{kl}S_{kl} + C_7\, \nu_T k/\varepsilon^2\, S_{ij}\Omega_{kl}\Omega_{kl}, \end{aligned} \tag{4}$$

$$\nu_T = C_\mu k^2/\varepsilon, \tag{5}$$

$$C_\mu = \frac{0{,}3}{1 + 0{,}35\left\{\max\left(\tilde{S}, \tilde{\Omega}\right)\right\}^{1{,}5}}\left[1 - \exp\left\{-0{,}36 \cdot \exp\left\{0{,}75 \cdot \max\left(\tilde{S}, \tilde{\Omega}\right)\right\}\right\}\right], \tag{6}$$

$$\tilde{S} \equiv \frac{k}{\varepsilon}\sqrt{\frac{S_{ij}S_{ij}}{2}},\ \tilde{\Omega} \equiv \frac{k}{\varepsilon}\sqrt{\frac{\Omega_{ij}\Omega_{ij}}{2}},\ S_{ij} \equiv \frac{\partial \overline{u}_i}{\partial x_j} + \frac{\partial \overline{u}_j}{\partial x_i},\ \Omega_{ij} \equiv \frac{\partial \overline{u}_i}{\partial x_j} - \frac{\partial \overline{u}_j}{\partial x_i},$$

where a_{ij} is the tensor of turbulence anisotropy; δ_{ij} is the Kronecker delta; ν_T is the eddy viscosity; k is the kinetic energy of turbulence; ε is the dissipation rate of kinetic energy of turbulence; $P = -\overline{u_i' u_j'}\,\frac{\partial \overline{u}_i}{\partial x_j}$ is the production of turbulent kinetic energy, $\sigma_k = 1$, $\sigma_\varepsilon = 1{,}3$, $C_{\varepsilon 1} = 1{,}44$, $C_{\varepsilon 2} = 1{,}92$, $C_1 = -0{,}1$, $C_2 = 0{,}1$, $C_3 = 0{,}26$, $C_4 = -10C_\mu^2$, $C_5 = 0$, $C_6 = -5C_\mu^2$, $C_7 = 5C_\mu^2$.

Quadratic combinations of ***S*** and Ω tensors take into account of the normal stresses anisotropy. Cubical terms are need for correct modelling of influence of streamlines curvature and flow swirling.

The inlet boundary conditions (B.C.) are based on wind-tunnel data; outlet and lateral B.C. are simple gradient conditions. The wall-function method [1] is used to describe interaction of flow with obstacles and solid surfaces.

The problem is solved numerically, and differential equations are discretized by the finite-volume method [5]. The convective terms of the transport equations are approximated with the use of MLU second-order scheme [7]. To calculate the integrals, piecewise-linear profiles, describing the function variation between nodes, are used. This discretization yields the grid equations, which are solved by the Buleev's explicit method of incomplete factorization [3]. To match the pressure and the velocity fields, Patankar–Spalding SIMPLE algorithm [5] is used. Calculation of parameters in the domain of complex geometry is executed within the method of fictitious areas.

The numerical simulation is based on the MUST experiment dataset (Figure 1). The main point of the experiment is to simulate the real urban obstacles and to measure the flow field and turbulence parameters in case of different meteorological conditions [6]. The study

area is a large domain 200 m × 200 m with array of containers 10 × 12, each of which has size 2,2 m × 2,42 m × 2,54 m. The only container has dimensions 6,1 m × 2,44 m × 3,51 m at the central area of the computational domain. The boundary conditions are: inflow – $u_1 = U_{ref}\left(z/8,78\right)^{0,16}$, $U_{ref} = 5,5\ \mathrm{m^1 s^{-1}}$; $k = 1,45\ \mathrm{m^2 s^{-2}}$; $\varepsilon = 0,2\ \mathrm{m^2 s^{-3}}$, $H_{ref} = 2,54\ \mathrm{m}$; outflow and lateral boundaries are $\partial\Phi/\partial n = 0$, where Φ is $u_1, u_2, u_3, k, \varepsilon$ and $\vec{n}$ is normal to boundary vector. We will consider the approaching flow perpendicular to the container arrangement.

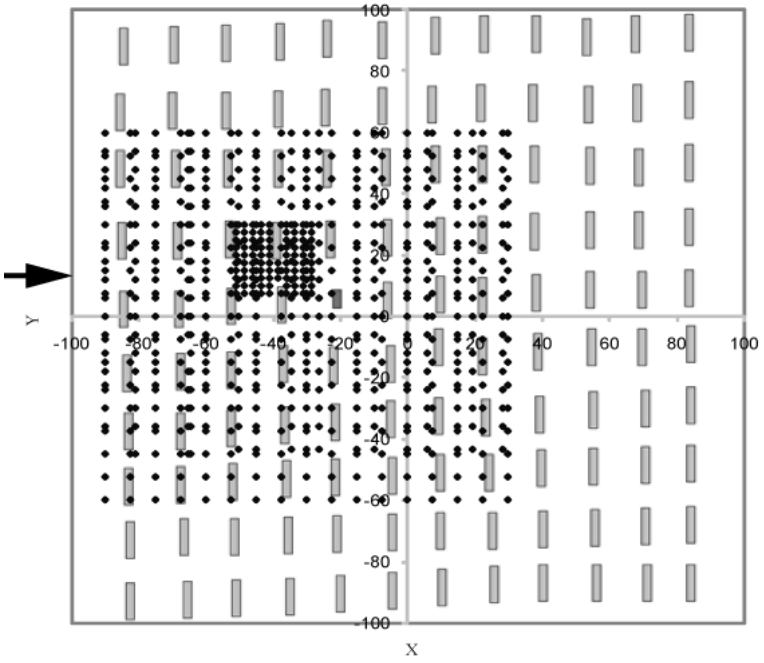

• - location of measurement points, the arrow is denote the wind direction

Fig. 1 – The scheme of computational/experimental domain for MUST.

3 Results

The developed model is evaluated on the basis of a metrics set which measure of model performance and usually applied for air quality models [6]. The following equations define these metrics, which include fractional bias (*FB*), Hit Rate (*q*), Correlation coefficient (*R*), Normal Mean Square Error (*NMSE*), and fraction of predictions with a factor of two of observations (*FAC*2):

$$FB = \left(\overline{O} - \overline{P}\right)/\left(0{,}5 \cdot \left(\overline{O} + \overline{P}\right)\right),\ \overline{O} = {}^{1}\!/_{n} \sum_{i=1}^{n} O_i\ ,\ \overline{P} = {}^{1}\!/_{n} \sum_{i=1}^{n} P_i\ ,$$

$$q = {}^{N}\!/_{n} = {}^{1}\!/_{n} \sum_{i=1}^{n} N_i\ ,\ N_i = \begin{cases} 1, \text{ for } \left|\left(P_i - O_i\right)/O_i\right| \le D \text{ or } \left|P_i - O_i\right| \le W, \\ 0, \text{ otherwise} \end{cases}$$

$$NMSE = \sum_{i=1}^{n} \left(O_i - P_i\right)^2 \Big/ \sum_{i=1}^{n} \left(O_i P_i\right),$$

$$R = \frac{\sum_{i=1}^{n}\left[\left(O_i - \overline{O}\right)\left(P_i - \overline{P}\right)\right]}{\left[\sum_{i=1}^{n}\left(O_i - \overline{O}\right)^2\right]^{1/2}\left[\sum_{i=1}^{n}\left(P_i - \overline{P}\right)^2\right]^{1/2}},$$

$$FAC2 = \text{fraction of data that satisfy } 0{,}5 \le P_i/O_i \le 2{,}0.$$

Here, P_i is the model predictions; O_i is the observations/experimental data; $\overline{P}$ is the average over the data set; N is the number of measurement points, D is the ratio error (=0,25) and W is the absolute error. A perfect model would have q, $FAC2$ = 1, and FB, $NMSE$ = 0. The metrics FB and $NMSE$ are used only for positive values (the kinetic energy of turbulence), because the negative variables could lead to inadequate results.

Table 1 – The metrics for vertical profiles of velocity and kinetic energy of turbulence

	Number of points	*W*	*D*	*R*	*q*	*FAC2*	*FB*	*NMSE*
u_1	566	0,008	0,25	0,83	0,70	0,90	-	-
u_3	566	0,007	0,25	0,59	0,17	0,17	-	-
k	566	0,005	0,25	0,39	0,43	0,79	0,38	0,35

A satisfactory model should have the following values of the mentioned above metrics [6]: 1) $FAC2 \ge 0{,}5$; 2) FB<0,3; 3) $NMSE$<4; 4) $q \ge 0{,}66$; 5) R>0,5.

The results of computations show that the hit rate for axial velocity u_1/U_{ref} is usually higher than 0,66 (Table 1). There is substantial disagreement of vertical velocity u_3/U_{ref} with experiment ($q = 0{,}17$). In spite of this the correlation coefficient R display that the developed model could satisfactory predict of averaged velocity profile. Figure 2 demonstrates that the underestimation of u_3 exists inside the array of containers and at the roof level.

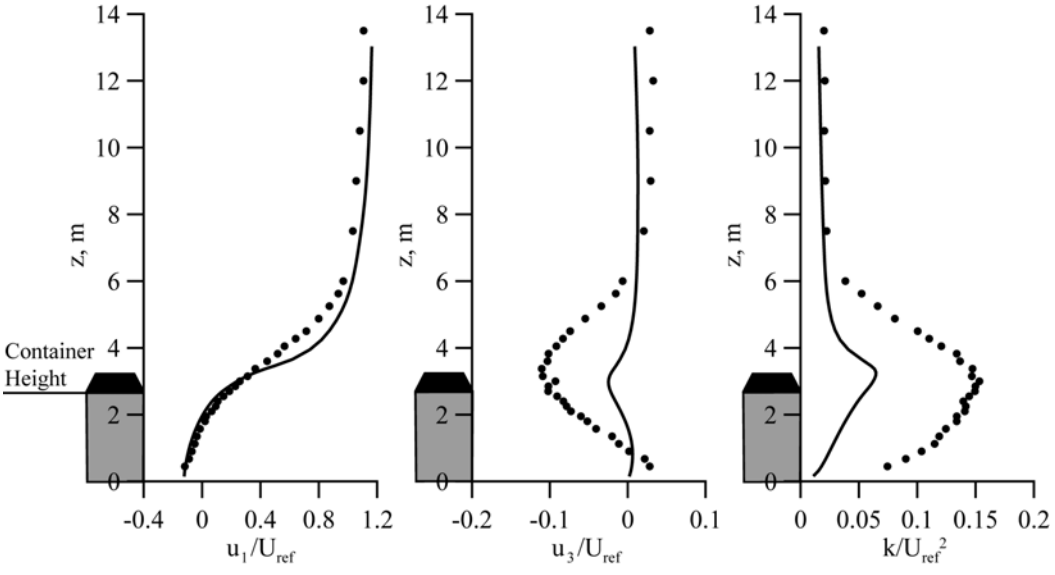

Fig. 2 – Vertical profiles of u_1, u_3 and kinetic energy of turbulence at $x = -76$, $y = 3$.

In accordance with the Table 1 there is also underprediction of the kinetic energy of turbulence k/U_{ref}^2 (positive values of *FB*), but parameter *FAC2* indicate that the part of such predicted data is less than 35%.

The averaged values are derived from computations in the following way [4]:

$$\langle \bar{\phi} \rangle_k = 1/N \sum_i \sum_j \bar{\phi}_{i,j,k} \,,\ \langle \overline{\phi' \psi'} \rangle_k = 1/N \sum_i \sum_j \left(\overline{\phi' \psi'} \right)_{i,j,k} \,,$$

$$\langle \tilde{\phi} \tilde{\psi} \rangle_k = 1/N \sum_i \sum_j \left(\bar{\phi}_{i,j,k} - \langle \bar{\phi} \rangle_k \right) \left(\bar{\psi}_{i,j,k} - \langle \bar{\psi} \rangle_k \right),$$

where the sum is performed over the *N* points that are within the air volume of the averaging volume at level *k*; *N* is equal to 16954 below *H* and 20020 above.

The dispersive kinetic energy is defined as:

$$\langle e \rangle = \frac{1}{2} \left(\langle \tilde{u}_1^2 \rangle + \langle \tilde{u}_2^2 \rangle + \langle \tilde{u}_3^2 \rangle \right).$$

To compute the drag coefficient C_D for a single canyon unit (air volume with the one container) the following relation is used [4]:

$$C_D = \frac{1}{u_1 |u|} \frac{\Delta y}{\Delta z N_{obs}} \Delta P_k \,.$$

Here, u_1 is the averaged velocity per canyon unit; Δz is the height of a container; Δy is the length of the container; N_{obs} is the number of grid cells per container and ΔP_k is the difference of pressure on the windward and the leeward sides of the container.

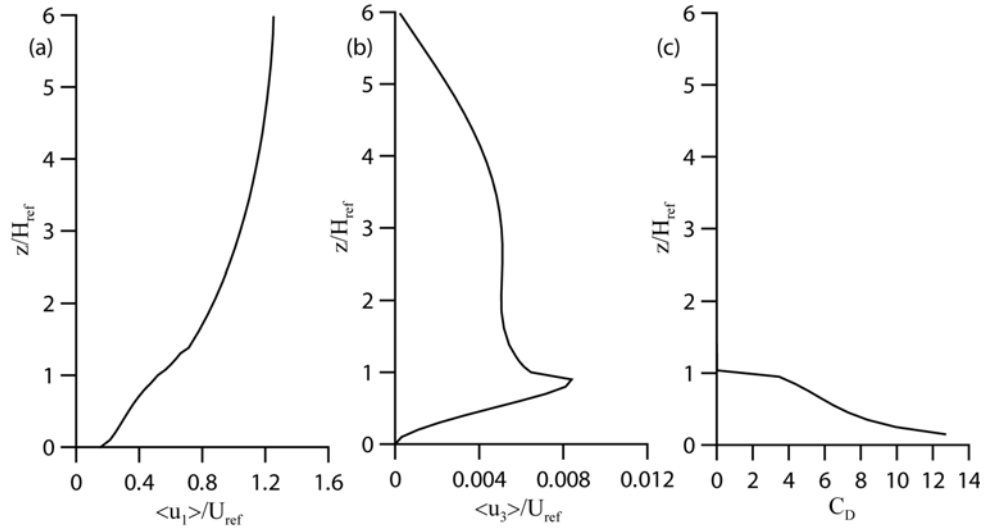

Fig. 3 – Vertical profiles of averaged variables: (a) mean axial velocity; (b) mean vertical velocity; (c) vertical profile of the drag coefficient (non-dimensional).

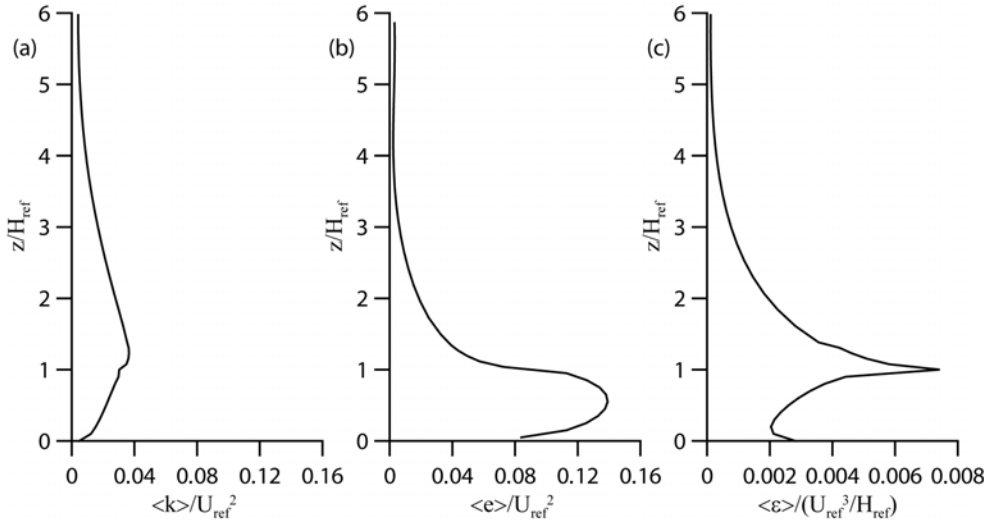

Fig. 4 – Vertical profiles of averaged variables: (a) kinetic energy of turbulence; (b) dispersive kinetic energy; (c) dissipation rate.

Vertical velocity profile of the mean u_1 component (Fig. 3) is approximately linear with height between containers. The results of averaging show that there is no logarithmic law at the roof level and above of containers. Such behavior of the wind profile is in contrast with the commonly used assumption of the log-law for urban canopy. The log-law will be present above the canopy in the case of regular arrangement of obstacles and for obstacles with the cubic shape [4]. There is weak advection in vertical direction (Fig. 3) in comparison with the horizontal transport. The drag coefficient is not a constant and it is substantially varied with height. It does not mean that there is not any similarity of such variation for different obstacles but values of C_D are depended on obstacles geometry and flow conditions.

In accordance with the results of simulation the turbulent kinetic energy $\langle k \rangle$ has maximum at the roof level and decreases inside and above the canopy while the maximum of the dispersive kinetic energy $\langle e \rangle$ is between the containers (Fig. 4). The maximum of dispersive kinetic energy is account for structures smaller that the size of the averaged volume (coherent canyon vortexes).

4 Conclusion

The analysis of the model performance on the basis of metrics was conducted. The results of the analysis indicate satisfactory quality of the model. The averaged velocity shows that the vertical profiles of velocity depend on geometry and arrangement of obstacles. Therefore, the profile of velocity is not always logarithmic for urban canopy. The dispersive kinetic energy is substantially higher than the turbulent kinetic energy in canopy. It means the importance of correct parameterization of dispersive stresses in NWP models because they have significant effect on total gradient of the sub-grid fluxes.

Acknowledgments. The study is funded by INTAS grant Ref. Nr. 06-1000016-5928 and RFBR grant Nr. 07-05-01126.

5 References

1. *Chieng, C.C., B.E. Launder* (1980) On the calculation of turbulent heat transport downstream from an abrupt pipe expansion. Numerical Heat Transfer, Vol. 3, pp. 189–207.

2. *Craft, T.J., B.E. Launder, K. Suga* (1996) Development and application of a cubic eddy viscosity model of turbulence. International J. of Heat and Fluid Flow, Vol. 17, pp.108–115.
3. *Ilin, V.P.* (1995) Methods of incomplete factorization for algebraic systems solving. Fizmatlit, Moscow, Russia, 288 pp.
4. *Martilli, A., J.L. Santiago* (2007) CFD simulation of airflow over a regular array of cubes. Part II: analysis of spatial average properties. Boundary-Layer Meteorology, Vol. 122, p. 635–654.
5. *Patankar, S.V.* (1980) Numerical heat transfer and fluid flow. Hemisphere Publishing Corporation, USA, 214 pp.
6. *Sabatino, S.D., R. Buccolieri, H. Olesen, M. Ketzel, R. Berkowicz, J. Franke, M. Shatzmann, H. Schlunzen, R. Britter, C. Borrego, A.M. Costa, S.T. Castelli, T. Reisin, A. Hellsten, J. Saloranta, N. Moussiopoulos, F. Barmpas, K. Brzozowski, I. Goricsan, M. Balczo, J. Bartzis, G. Efthimiou, J.L. Santiago, A. Martilli, M. Piringer, M. Hirtl, A. Baklanov, R. Nuterman, A. Starchenko* (2008) COST 732 in practice: the MUST model evaluation exercise. Accepted for publication in Int. J. of Environment and Pollution, 8 pp.
7. *Van Leer, B.* (1974) Towards the ultimate conservative difference scheme. II. Monotonicity and conservation combined in a second order scheme. Journal of Computational Physics, Vol. 14, pp. 361–370.
8. *Wilcox, D.C.* (2006) Turbulence Modelling for CFD. DCW Industries, Inc., La Canada, California, 522 pp.

Применение микромасштабной модели для разработки схемы параметризации городской застройки в мезо-масштабных моделях

Аннотация. *Численное моделирование течений в условиях городской застройки является важным при обеспечении готовности к аварийным ситуациям, а так же для разработки новых схем параметризации атмосферного пограничного слоя в численном прогнозе погоды. Данное исследование представляет собой анализ свойств потока, осредненных по пространству, вокруг различных препятствий характерных для города.*

Ключевые слова: *микромасштабная модель с явным выделением препятствий, параметризация городской застройки.*